

# UNCLASSIFIED

Approved for Public Release; Distribution is unlimited.

## Aero-optical Demonstration Test in the AEDC Hypervelocity Wind Tunnel 9\*

Dan Marren†

Arnold Engineering Development Center/White Oak  
10905 New Hampshire Ave.  
Silver Spring, MD 20905-1050

### Abstract

Hypersonic endo-atmospheric interceptors must maneuver over a variety of flight environments. Generally, these interceptor missions require flight below Mach 8 for some portion of the mission. Hypervelocity intercepts can occur at high altitudes but are more stressing at the lower altitude, high Reynolds number conditions.

To obtain the high accuracy needed for hit-to-kill, endo-atmospheric interceptors use optically based seeker systems. These optical seekers rely on precise knowledge of the interceptor position to select an aimpoint. Optical aberrations caused by hypersonic flight can distort or shift the image position on the focal plane enough to add uncertainty in the position and cause the interceptor to miss. These image distortions are typically referred to as aero-optical effects.

To lower risk to the program, the thermal and structural response and the optical aberrations on the seeker window should be assessed through ground testing. This type of ground testing is dependent on duplicating flight parameters. In addition, thermal/structural testing requires long run times consistent with end-game scenarios. Evaluation of interceptor performance in a ground test facility that can provide full flight duplication for seconds of run time will greatly reduce risk to these programs.

An aero-optics test capability has been demonstrated in Hypervelocity Wind Tunnel 9 (Tunnel 9) at the Arnold Engineering Development Center (AEDC). In this facility, flight aerodynamic conditions can be matched for run times of 6 seconds,

thereby duplicating the aerothermal/structural response of the window. This facility creates an ideal environment to characterize and evaluate seeker system aero-optical effects. This paper outlines the significant verification and validation processes developed for feasibility demonstration. It provides an overview of the important aspects and results of the program to date. It describes the stages of detailed calibration performed validating the instrumentation for use in a world-class ground test facility, and highlights the first aero-optical data taken in a Mach 7 thermal/structural environment.

### Introduction

Aero-optic measurements have been investigated in hypersonic test facilities since the early 1970's when optical seekers began to enter technological feasibility. Tunnel 9 (under Navy direction) and AEDC Tunnel C engineers have investigated the challenge of precise aero-optic measurements. In fact, the first aero-optic measurements in a hypersonic facility were made at Tunnel 9. Additionally, recent aero-optical testing has been completed at the LENS shock tunnel in Buffalo, NY. Due to the limitations of shock tunnels (run times less than 20ms), only the flow-field portion of aero-optics is obtained. The aerothermal and thermal/structural effects cannot be duplicated. Therefore, a complimentary capability that duplicates the thermal/structural environment, while providing the aero-optical characteristics of the seeker geometry, is critical for the understanding of the complete aero-optic phenomenon.

Two recent advancements have been introduced that now permit the measurement of the important aerothermal/structural characteristics of

\* The research reported herein was performed by the Arnold Engineering Development Center (AEDC), Air Force Materiel Command. Work and analysis for this research were performed by personnel of Sverdrup Technology, Inc., AEDC Group, technical services contractor for AEDC. Further reproduction is authorized to satisfy needs of the U. S. Government.

† Senior Member, AIAA.

This paper is declared a work of the U. S. government and not subject to copyright protection in the United States.

# UNCLASSIFIED

a seeker window. First, the facility enhancements to Tunnel 9 permit environment duplication of flight at Mach 7 on full-scale interceptor hardware at low altitude (10-20km) for representative flight times (6 seconds). This facility can now reproduce the physical environment needed to create thermal gradients and deform seeker windows. The second advancement is the application of a Shack-Hartman type sensor to the instrumentation suite. This sensor can capture a statistically significant (30-120hz) sample of the phase and intensity of an incoming light beam, which enables the calculation of aero-optic parameters of interest.

## History

Aero-optical testing at AEDC facilities has a long history dating back to the first aero-optical experiments in a hypersonic environment.<sup>1</sup> Subsequent Tunnel 9 and Tunnel C<sup>2</sup> tests were completed with some success in those initial years when aero-optical instrumentation and techniques were first being developed. In all the experiments however, certain challenges prevented obtaining the precise aero-optics measurements needed for seeker window evaluation. The measurements completed in Tunnel 9 contained a large amount of mechanical vibration from the facility operation and hardware limitations. The measurement uncertainty was too large (>50 micro-radians). The measurements made in Tunnel C also had vibration issues and there were optical distortions introduced by the facility windows, which heated up during the test period adding measurement error to the overall system capability. Since that time it has been postulated that obtaining optical measurements in a wind tunnel with long run times (on the order of seeker end games), would be impossible or impractical. Optical measurements were then obtained in a shock tunnel to make use of the extremely short run times, attempting to capture all the flow-field optical data before the mechanical energy could reach the optical setup. This approach was beneficial for providing the flow-field component of the aero-optical phenomenon but did not duplicate the thermal time-dependant optical aberrations induced by high-speed flight.

In 1995, a modification to the Tunnel 9 facility was made. This upgraded capability duplicates the

end-game aerothermal environment for endo-atmospheric interceptor systems providing duplication of the environment for up to 6 seconds of test time accommodating full scale interceptor kill-vehicle forebodies and windows.<sup>3</sup> The Tunnel 9 Mach 7 thermal/structural facility was developed and in 1996, tested a full-scale Theater High Altitude Area Defense (THAAD) kill vehicle for structural testing of the windows prior to flight.<sup>4</sup> This highlighted the need for a facility enhancement to be developed which could simultaneously obtain the optical performance data during this thermal and structural testing.

## Wavefront Sensor

The optical suite is built around an instrument called the Shack-Hartmann wavefront sensor (WFS) developed by Wavefront Sciences Corporation in Albuquerque, NM. This device provides all wavefront phase and intensity information at sample speeds currently between 30-120Hz. Detailed information concerning the Shack-Hartmann wavefront sensor can be found in Ref. 5.

The WFS was developed initially for adaptive optics, with the Air Force Phillips Laboratory, MIT Lincoln Laboratory, Sandia National Laboratories, and numerous universities playing a role. These sensors are robust, reliable, stable, and have large dynamic range and high sensitivity. They have been used extensively for adaptive optics as well as optical metrology and laser beam characterization.

The Shack-Hartmann principle is simple and is based on two concepts. Namely, light travels in a straight line in homogeneous media, and the optical wavefront is the surface normal to the direction of propagation. The WFS uses a lenslet array to spatially divide the incoming light among a large number of sub-apertures, and then measures the wavefront slope over each subaperture. The slope information is used to reconstruct the incident wavefront. The technology of wavefront reconstruction and analysis has been extensively developed, and can be applied to the design of sensors for measurement applications. The WFS combines a compact package with fast measurement and large dynamic range.

UNCLASSIFIED

# UNCLASSIFIED

All of the information is obtained in a single measurement that can be gated for a fraction of a second. It is robust, vibration insensitive, extremely accurate and easy to use. The sensor spatial resolution is determined by the lenslet size and spacing. The sensitivity is determined by the minimum detectable change in focal spot position (based primarily on detector noise and geometry). Dynamic range is limited by spot overlap.

Wavefront Sciences of Albuquerque, NM has designed two specific WFS for application in the Tunnel 9 hypersonic environment for use in these experiments. Table 1 shows the technical specifications of the two WFS (model 9701/6701) used in our experiments.

Table 1. Wavefront Sensor Technical Specifications

Parameter	9701 WFS	6701 WFS
Array Size	764 × 480	648 × 484
S/N	50dB	50dB
Framing Rate	30Hz	60Hz
Integration Time	1/16,000 s	1/32,000 s
Lenslet Array FL	25mm	8.2mm
Areas of Interest	35 × 26	37 × 30

## Aero-Optical Development Program

The approach for the development is to design a group of experiments that represent the physics of current interceptor systems. It is critical that these data can be validated with CFD and provide the right measurements to separate the optical effects of the aerodynamic flow field and the thermal/structural response. The overall development strategy is to follow the same methodology that would be used to design an interceptor seeker window. Figure 1 is a flow diagram of analysis schemes required in designing a seeker win-

dow system. It provides the basis for our data utilization plan and helps define the steps or phases in the demonstration.

The baseline program has four parts, a calibration/integration and three distinct Phases. The goal of the calibration phase was to verify that the instrument could be operated and integrated in the laboratory. The Phase 0 goal was to obtain environmental data on the instrument and the facility in order to maximize the optical suite design for the necessary measurements. The main objective was to answer the following two questions: (1) is the environment stable and quiet enough to make optical measurements? and (2) Can the target be introduced without distortion so that optical measurements are worthwhile?. The objectives of the Phase 1 effort are to demonstrate that, within performance criteria set based on seeker-design requirements, an undistorted target beam can be introduced into the test section over the entire six sec test duration, and that our instrumentation suite is capable of characterizing that target beam within those same criteria to make optical measurements on representative uncooled interceptor window geometry.

The Phase 2 objective is to demonstrate development of the full capability needed to characterize performance of actively-cooled windows. When complete, the instrumentation suite will be able to assess all types of optical seeker systems.

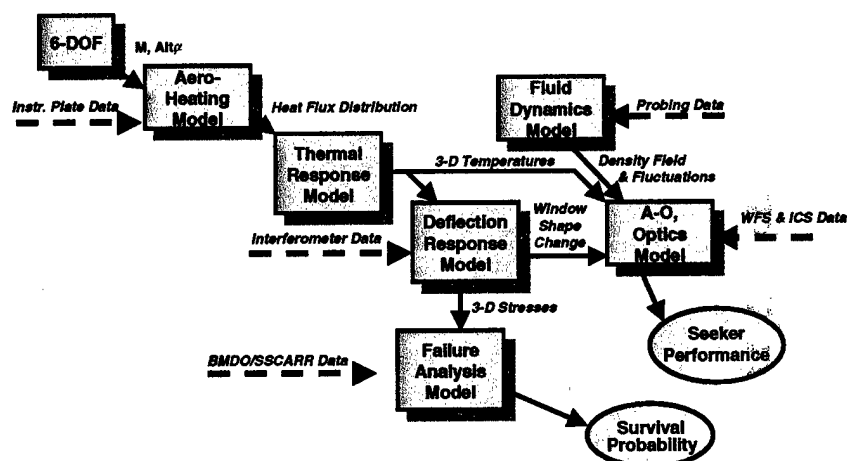


Fig. 1. Data Utilization Plan.

## Selection of Test-bed Geometry

The selection of model geometry was such to replicate the physical parameters related to BMDO endo-atmospheric interceptor geometries using optical seekers. Since there are varying requirements for each program, the geometry was chosen to replicate the physics associated with systems requiring active cooling for the window and those without cooling. Another important criterion for this test bed was to allow the calculation, prediction, and separation of effects due to aerodynamic, thermal and structural loading. The selected testbed configuration was a 15-degree wedge configuration with a sapphire window in a titanium frame as the seeker window. Figure 2 shows the test bed geometry while Fig. 3 shows the important features of the window/frame combination. The window and frame design represents the latest technical information concerning sapphire windows. Figure 4 shows the testbed mounted in the Mach 7 facility. Shown also in the photo is the opposing flat plate used to introduce the target beam to the test section. An identical window and frame combination was used in the target source plate due to the high thermal loads in Tunnel 9. The setup of the hardware in the facility could be mounted with both plates at 0 degrees incidence to the flow for calibration purposes, or with one plate acting as the interceptor test bed inclined at 15 deg.

## Pre-test Analysis and Computational Predictions

Prior to the test series, computational predictions were made for the purpose of both design of

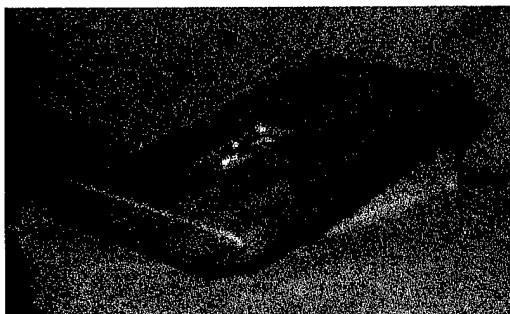


Fig. 2. T9 Aero-optical testbed.

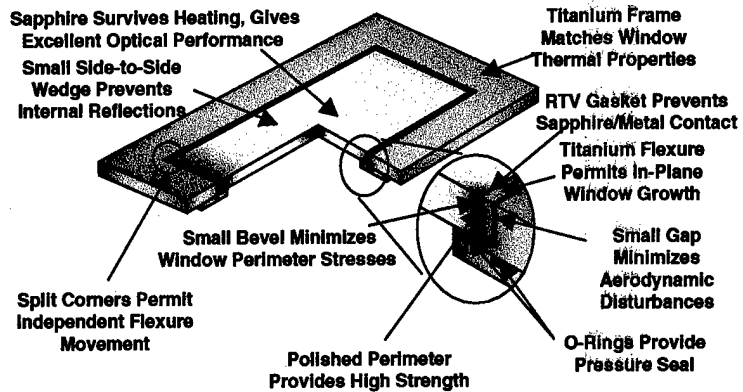


Fig. 3. Window and frame design.

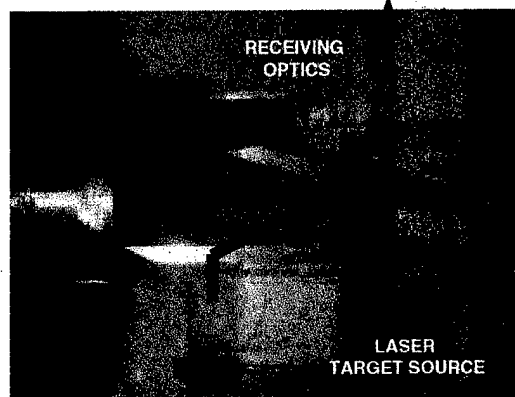


Fig. 4. Optical testbed installation.

the testbed and correlation of the integrated effects with the data set obtained. Throughout the course of the program, multiple computational solutions were performed. Figure 1 indicates the various types of computational solutions and their relation to test data required. Data plots will refer where applicable to the computational solutions. The detailed techniques and computational solutions are not the subject of this work and will be presented under separate titles.

## Pre-test Calibration and Integration

Tunnel 9 is a production test and evaluation facility, therefore, verification and validation (V&V) for every measurement is required. This was accomplished through careful calibrations representing the magnitude of optical aberrations that the window would experience during the test. The philosophy of the integration effort was to ensure the optical suite was sensitive to aero-optic parameters of interest. These parameters include window

UNCLASSIFIED

heating and coolant effects as measured by the quantities of blur, bore-sight error (BSE) and Strehl ratio. Separate calibration efforts reproduced the quantities of wavefront tilt, blur, and waves of distortion.

In order to obtain the most accurate optical measurements, the entire set up (suite) was first assembled in the calibration building and the system was built up on breadboards shown schematically in Fig. 5. In this manner, the accuracy of the instrument and of the suite could be determined without the environmental factors associated with running the facility. The instrument "noise floor" was determined to be  $\pm 2$  micro-radians of wavefront tilt with a beam quality of 1.1 times diffraction limited point spread function. Several measurement calibration schemes were used in this effort. Each test calibrated the suite for a different optical parameter and was valid over a certain range. Table 2 shows the specific calibration test and its relation to the overall seeker data required.

## 1. Curvature Tests

During integration tests, a predicted window deformation was applied to the laser input to measure the blur and Strehl sensitivity and to accurately characterize the optical suite. Curvature radii varied from 12.1 m to infinity. In this way, the WFS and the ICS can be compared to theoretical values of curvature. All the sensor data was essentially co-incident. Results of the curvature tests are shown in Fig. 6.

## 2. Aperture Tests

During the aperture tests, the primary aperture was set to four different sizes between 2.2 mm and 6.2 mm in diameter. Figure 7 shows the result of these experiments. In all cases, the data sets exactly over-layered each other.

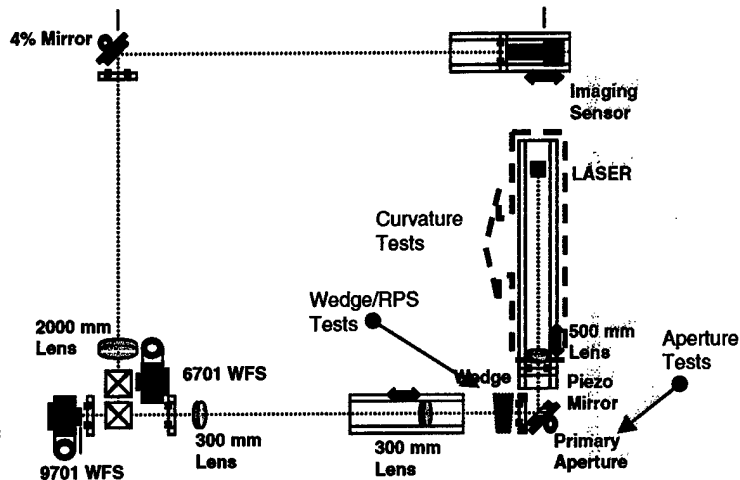


Fig. 5. T9 integration and verification bench setup schematic.

Table 2. Calibration Schemes and Relation to Interceptor Type

Measurement	Uncooled Window	Cooled Window	Integration Effort
BSE	Low	High	Wedge/Curvature/RPS
Blur	Low	High	Curvature/RPS
Strehl	High	Range	Aperture/RPS
Deformation	High	High	Curvature
s	Low	High	RPS
l <sub>c</sub>	Long	Short	RPS

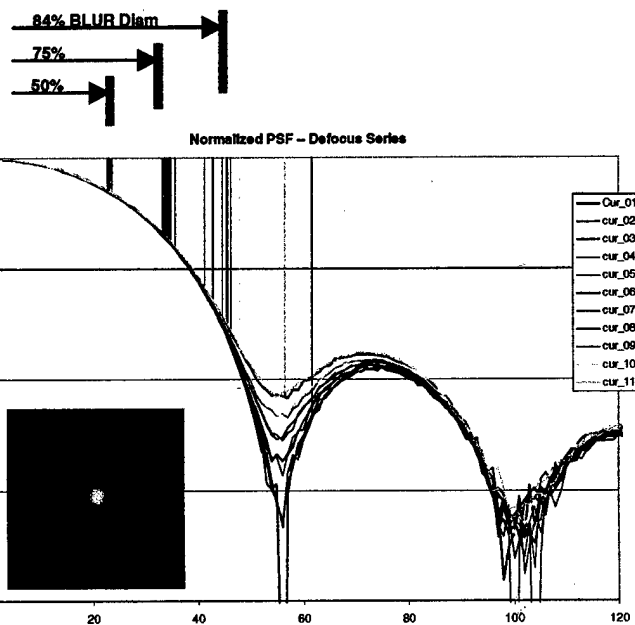


Fig. 6. Curvature calibration results.

UNCLASSIFIED

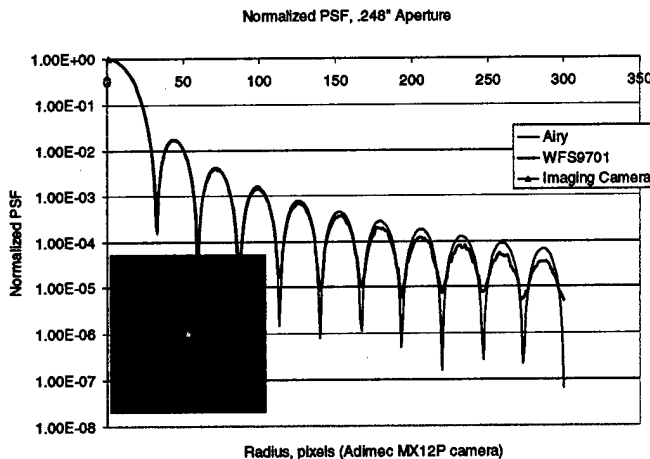


Fig. 7. Aperture calibration results.

### 3. Wedge Tests

During the wedge tests, a precision optical wedge was placed in front of the primary aperture. The wedge introduces a known 248.1 micro-radian tilt to the incoming wavefront. This can be used to calibrate the tilt or BSE by placing the wedge at different orientations and calculating the resulting tilt for attitude. Figure 8 shows the results of the wedge calibration. The RMS error in the calibration was calculated at less than two micro-radians.

### 4. Random Phase Sheet Tests

Using numerical simulation, a phase screen was developed to describe the phase delay introduced by propagation through various levels of tur-

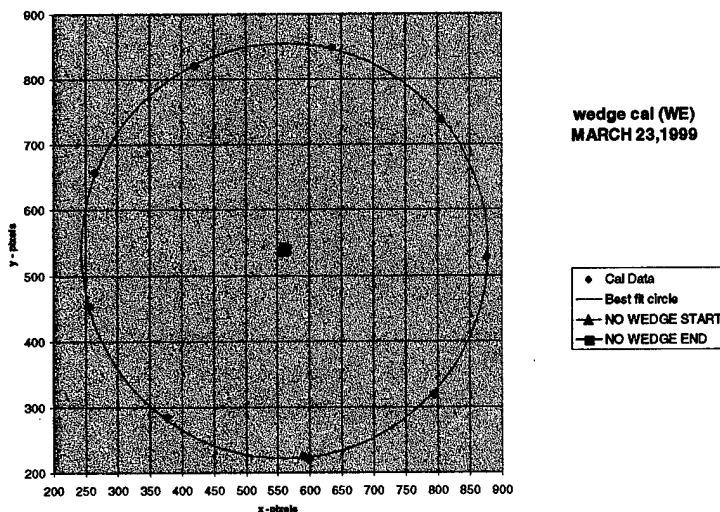


Fig. 8. Wedge calibration results.

bulence. The simulation allowed for several look angles and turbulence strengths as defined by the characteristic length ( $l_c$ ) and ratio ( $\sigma$ ). The phase screen data was used to create a micro-optic to impose the appropriate phase structure on the light passing through it. The random phase sheet was placed at the primary aperture. Four zones on the sheet were illuminated. The distorted wavefront was collected by all sensors. Each of the zones represents turbulence levels much higher than would be produced by an interceptor coolant system. Figure 9 shows a comparison of point spread functions for both the WFS and Imaging Camera System (ICS). Excellent agreement is demonstrated even with the introduction of extreme turbulence levels.



WFS and Imaging Camera Observe Zone 1 of a Random Phase Sheet. PSFs from the WFS were Computed Analytically from the measured intensity and phase in the near field. The Image Camera Observes PSFs directly.

Fig. 9. Random phase sheet calibration results.

### Tunnel 9 Facility Description and Operation

Tunnel 9 is located at the White Oak, MD site of AEDC. It provides clean, uniform aerodynamic flow fields at high Reynolds numbers with long run times. Tunnel 9 has played a major role in the testing of reentry systems, endo-atmospheric interceptors, and aerospace plane programs. Specific testing areas include aerodynamics, high-speed inlets, aerothermal heating, jet interaction, and shroud removal.

Tunnel 9 is a blowdown facility that currently operates at Mach numbers of 7, 8, 10, 14, and 16.5. Tunnel 9 uses

pure nitrogen as the working fluid. The test section is over 12 feet long and five feet in diameter, which enables testing of full-scale model configurations. A layout of Tunnel 9 is shown in Fig. 10. Ranges for Reynolds numbers and supply conditions are listed in Table 3.

During a typical run, a vertical heater vessel is used to pressurize and heat a fixed volume of nitrogen to a predetermined pressure and temperature. The test section and vacuum sphere are evacuated to approximately one mmHg and are separated from the heater by a pair of metal diaphragms. When the nitrogen in the heater reaches the desired temperature and pressure, the diaphragms are ruptured. The gas flows from the top of the heater, expanding through the contoured nozzle into the test section at the desired test conditions. As the hot gas exits the top of the heater, cooler nitrogen from three pressurized driver vessels enters the heater base. The cold gas drives the hot gas in a piston-like fashion, thereby maintaining constant conditions in the test section during the run. A complete description of the current Tunnel 9 capabilities can be found in Ref. 6.

This test series was performed in the Mach 7, thermal/structural test capability, which duplicates the harsh environments experienced by endo-atmospheric interceptors. Run times on the order of un-shrouded

end game times at full flight duplication provides the thermal exposure needed for full-scale seeker window testing. The Mach 7 facility utilizes the high pressure and temperature capability in the Mach 14 heater but expands the flow to a Mach number of 7, concentrating the high enthalpy flow in a smaller, high energy nozzle core flow. This Mach 7 flow maintains high pressure and temperature providing full flight duplication. Table 4 lists the performance parameters for the Mach 7 facility. Refs. 3 and 7 provide a complete description of the Mach 7 facility and calibration.

Table 3. Tunnel 9 Nominal Capabilities

Contoured Nozzle	PO Range, atm	T0, K	RE# Range, $\times 10^6/m$	Run Time, sec
7	177-805	1923	12-52.5	1-6
8	68-818	867	14.7-164	0.33 to 5
10	34-955	1006	2.8-65.6	0.23 to 8
14	6.8-1364	1784	0.2-12.46	0.7 to 15
16.5	1432	1856	10.6	3.5

Table 4. Mach 7 Thermal/Structural Facility Nominal Performance Parameters

Supply		Test Cell			Performance		
P0, atm	T0, K	Q <sub>Int</sub> , Kpa	T <sub>Int</sub> , K	P <sub>Int</sub> , Kpa	Run Time, sec	Vel, m/sec	Alt, km
177 - 805	1922	90 - 730	217	2.8 - 23	1 - 6	2188	10 - 20

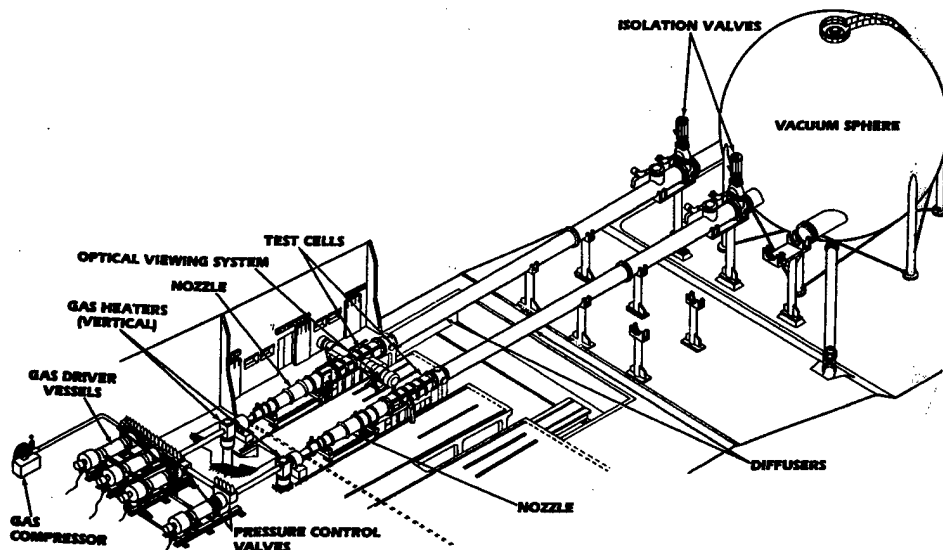


Fig. 10. AEDC Hypervelocity Wind Tunnel 9 Facility.

## Instrumentation and Measurements

The goal of the instrumentation suite is to make the right measurements to completely characterize the environment and window so that the various components of the optical aberrations can be separated and analyzed. The aerodynamic flow field, mechanical environment, local window environment and physical characteristics such as window heating, window deformation, and all optical transmissive properties of the window must be simultaneously obtained as functions of time. The instrumentation suite is designed to obtain data in the following six areas: (1) surface pressure and temperature, (2) infrared thermography, (3) back-face window temperatures (4) window deformation, (5) shear/coolant layer flow-field probes, and (6) line-of-sight redundant optical measurements. Each data input from the optical suite relates the overall data utilization plan as shown in Fig. 1.

### Tunnel Aerodynamic Environment and Local Flow Field

For the first two runs, the sapphire window was replaced by a metal plate to fully characterize the window environment. Measurements proved the facility environment to be very repeatable as Fig. 11 shows twelve runs plotted as a function of time. The high degree of repeatability within 2 percent from run to run enables the results from one run to be compared to a subsequent run.

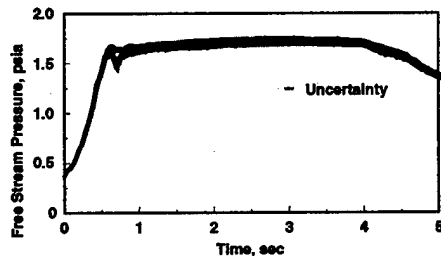


Fig. 11. Free-stream repeatability data.

Measurements were also made on the wedge surface leading up to the window region and in the window area itself. Figures 12 and 13 show pres-

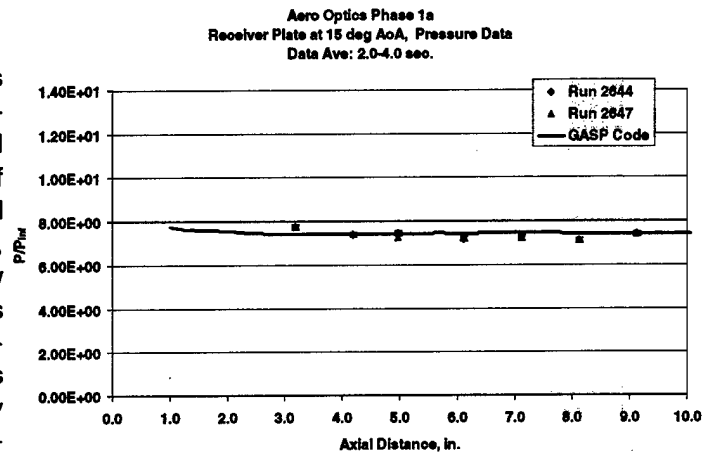


Fig. 12. Local environment pressure profile.

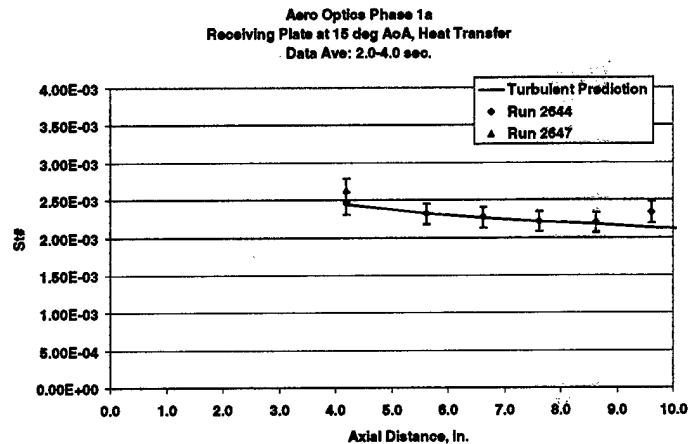


Fig. 13. Local environment temperature profile.

sure and temperature profiles of the region where the window is to be inserted. In each case the local aerodynamic environment is uniform and repeatable and compares well with the predictions of a wedge flow field. Similar measurements were made with the sapphire window in place. The installation of conventional thermocouples on or in the window could have changed the structural response and thermal characteristics of the window; therefore, they were not used when testing the sapphire windows. Instead, infrared thermography was obtained for the window surface to determine the uniformity of surface heating, gasket/seal leaks, and to verify heat conduction modeling. Figure 14 shows an IR image of the target source window in the flow field. Notice the uniform low heating, which aids in the introduction of a clean target. Figure 15 shows the measured back face tempera-



ture of the sapphire window as a function of time while inclined at 15 degrees. The thermocouples used for this measurement were type "E" foil thermocouples mounted on a spring-loaded pad and pressed to the back of the window. The thermocouples were held with just enough pressure to insure contact with the sapphire surface. Back face temperature rise measurements again compare well with pre-test predictions.

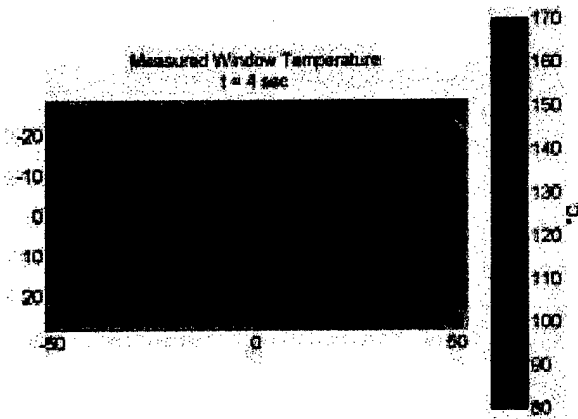


Fig. 14. Infrared front face temperature map.

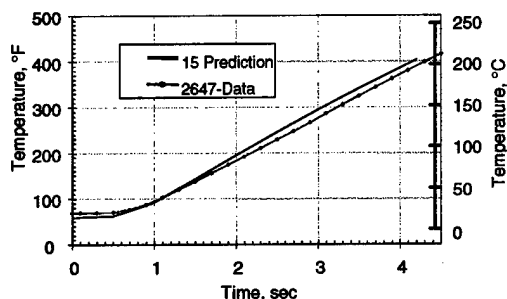


Fig. 15. Back face temperature rise 15 deg plate.

## Mechanical Vibration Monitoring

Since part of the feasibility demonstration was to characterize the mechanical vibrations introduced by the facility itself, measurements were obtained to characterize the mechanical energy magnitude and frequency. The suite has the capability to actively measure and characterize the mechanical environment during a test program or tunnel run. Since the facility runs for multiple seconds, it is important to characterize and understand the mechanical environment present to obtain measurements within the stated accuracy of the optical suite.

Tri-axial and angular accelerometers were recorded at various stations around the optical benches and on optical mounts. Fig. 16 shows the layout of accelerometers in relation to the optical table. In addition, a high sample speed (15-55 kHz) X-Y detector was used to image the coincident beam path as the primary optical sensors. In this manner we were able to de-convolve the mechanical energy paths, attribute the unacceptable levels of vibration to a specific component and correct any sources of mechanical noise for the final configuration. A detailed modal analysis was completed prior to the test entry to identify energy paths through the entire optical system.

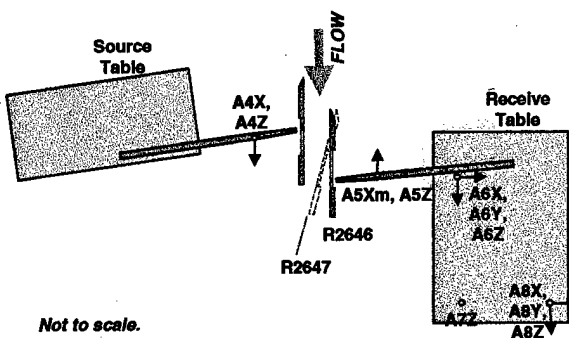


Fig. 16. T9 mechanical monitoring system setup.

## Optical Measurements

The optical instrumentation suite was designed to capture all the optical properties of the wavefront as it passes through the seeker window during the flight duplicated test times. The optical setup is shown in Fig. 17. Two optical tables are placed at either side of the facility adjacent to the test sec-

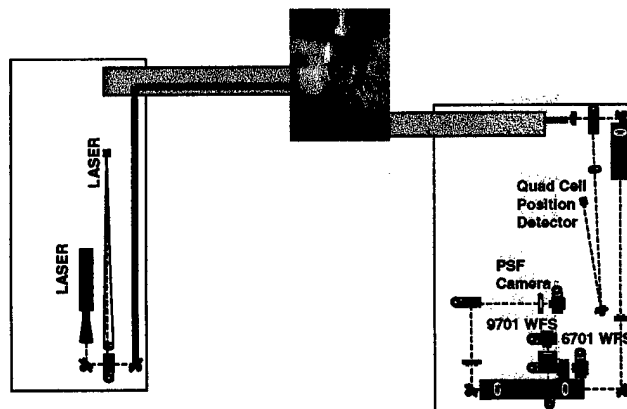


Fig. 17. T9 aero-optical suite testing setup schematic.

tion. One optical bench contains a target source laser and the other table contains all the collection optics. The laser target source is introduced through a light tube into the target source window. Steering mirrors turn the beam and direct it toward the test bed window and into another light tube and through to the receiving side collection optical components.

For the demonstration phase, a He-Ne laser, operating at a 633 nm wavelength, was used as the target source. This signal was imaged to the receiving optics and imaged to multiple sensors. Two wavefront sensors, described in the previous section, represent the primary measurement. In addition, simultaneous redundant instrumentation was used to independently verify operation and accuracy of the primary sensor. An imaging camera and quad cell X-Y detector were used to image the beam simultaneously. Table 5 lists the measurement accuracy goals of this phase of testing in relation to the actual performance observed for the optical properties of interest.

Optical data were obtained and are shown in Figs. 18-21. Raw data from the wavefront sensor and the calculated centroid positions in two dimensions are shown in Fig. 18. The point-spread function (PSF) is then calculated for each point in time and is shown for an instantaneous sample in Fig. 19. The PSF is then compared directly to the ICS system as shown in Fig. 20. This provides independent measurements of the optical quantities during the test for verification purposes. As the window is heated aerodynamically, during the 4.5-second run, it deforms and the BSE shift is evident until the

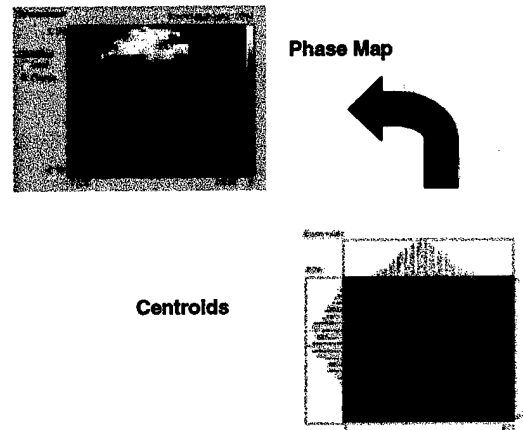


Fig. 18. Raw wavefront sensor data.

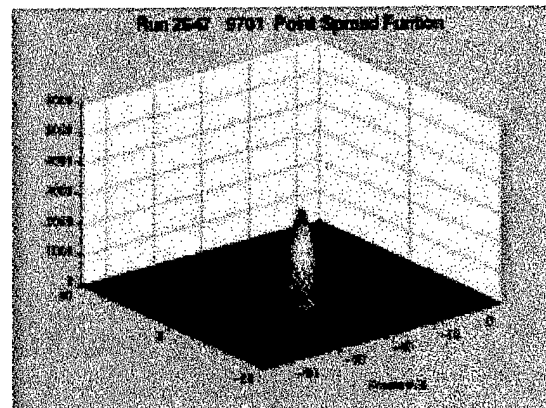


Fig. 19. 2-D PSF representation from 9701 WFS.

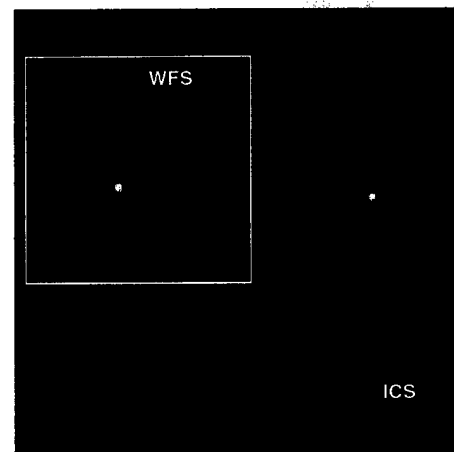


Fig. 20. Comparison of PSF for WFS and ICS.

Table 5. Tunnel 9 Aero Optics Demonstration Objectives

Parameter	Acceptable Minimum	Near Term Objective	Achieved to Date
BSE Uncertainty	$\pm 15 \mu\text{rad}$	$\pm 10 \mu\text{rad}$	$\pm 15 \mu\text{rad}$
# Instantaneous Wavefronts	> 40	> 300	100
Measurement Time $\Delta t$	< 500ns	< 250ns	10 ns
Tare PSF Quality	1.5X DL	1.4X DL	1.1X DL
Local Str hal # ( $\Delta t + U_c/L_c$ )	< 0.5	< 0.25	0.01
% Encircled Energy	< 30%	< 15%	25%
# Samples in 1D Slice	12	25	45

UNCLASSIFIED

window is allowed to cool to the pre run levels. Figure 21 shows the effect of the thermal environment on the window and the resulting change in the average tilt or BSE. The total jitter induced by facility operation is within  $\pm 14$  micro-radians. Thermal and structural loading result in an increased tilt in both X and Y dimensions.

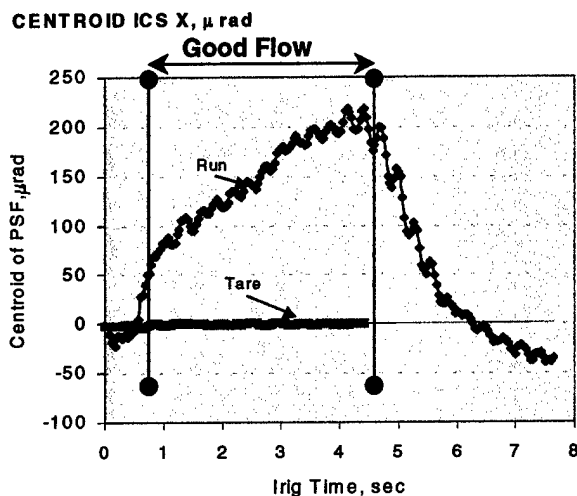


Fig. 21. Average tilt in the X direction for entire run sequence on the 15 deg testbed.

### Summary

The AEDC Hypervelocity Wind Tunnel 9 has demonstrated the minimum acceptable performance goals for the demonstration. The capability to obtain high quality, aero-optical data in flight-duplicated conditions for actual interceptor missions will be demonstrated in the next phase during the summer of 1999. The 4-6 second test duration allows for the measurement of the aerodynamic, thermodynamic, thermal structural and optical response simultaneously. Prior challenges relating to vibration and thermal effects from the facility have been shown to be within acceptable tolerance levels and are manageable. The target spot quality presented to the interceptor is stable, repeatable and of high quality (1.1 DF). Facility induced total noise is below  $\pm 15$  micro-radians and is suitable for interceptor seeker window testing.

The first phase of the aero-optics demonstration has been successfully completed. The next step is

to measure direct optical properties of the window under these calibrated conditions and separate the optical effects due to thermal heat soak from the aerodynamic effects. Once these results are verified, a slot cooled geometry can be tested to demonstrate the ability to characterize all types of optically guided seeker windows.

When complete, Tunnel 9 will be capable of testing all types of seeker window systems in an environment that provides both the thermal structural and the aero-optical effects on survivability and seeker performance. Program inputs will be re-addressed to verify that the test data produced during the next phase of testing integrates into the test and evaluation process of each program.

### Acknowledgements

The author would like to acknowledge the dedication and hours of hard work by the individuals responsible for the technical design, development, and test conduct related to each subsystem involved in this demonstration. This effort required the successful integration of a team of individuals from four organizations with the skills necessary for this effort.

#### AEDC/White Oak, Silver Spring, MD

A. Collier, J. Lafferty, W. C. Spring, W. Yanta and G. Wannenwetsch and the T9 Operations Crew.

#### Sverdrup Tech. Inc. Arnold Air Force Base, TN

T. Hartvigsen and B. Bertrand.

#### Sy-Technology, Huntsville, AL

M. Banish, R. Cayse, D. Chenault, R. Crouse, E. Rawlinson and R. Shaw.

#### Wavefront Sciences, Albuquerque, NM

D. Neal and D. Armstrong.

The author would also like to thank BMDO/TOT and the members of the individual BMDO programs for the definition of requirements for the optical suite.

UNCLASSIFIED

# UNCLASSIFIED

## REFERENCES

1. Hedlund, Eric R., Endoatmospheric Interceptor Test Capabilities in the NSWC Hypervelocity Tunnel #9, AIAA 92-2758, Huntsville, AL, May 1992.

2. Havener, G. and Stepanek, S., Aero-Optics Testing Capabilities at AEDC, AIAA 92-0760, Reno, NV, January 1992.

3. Marren, Dan E., Full Scale Thermostructural Wind Tunnel Test of the THAAD Seeker Window, 7th DoD Electromagnetic Windows Symposium, Laurel, MD, May 1998.

4. Henneman, L., et al, Full Scale Thermostructural Wind Tunnel Test of the THAAD Seeker Window, 7th DoD Electromagnetic Windows Symposium, Laurel, MD, May 1998.

5. Neal, Dan, Shack-Hartmann Wavefront Sensor Testing of Aero-optic Phenomenon, AIAA 98-2701, Albuquerque, NM, June 1998.

6. Boyd, C. and Ragsdale, W. C., Hypervelocity Wind Tunnel 9 Facility Handbook, Third Edition, NAVSWC TR 91-616, Silver Spring, MD, December 1991.

7. Lafferty, John F. and Marren, Dan E., Hypervelocity Wind Tunnel No. 9 Mach 7 Thermal Structural Facility Verification and Calibration, Technical Report NSWCDD/TR-95/231, Naval Surface Warfare Center, Silver Spring, MD 20903-5640, June 1996.

UNCLASSIFIED